PROCEEDINGS OF SCIENCE

A Numerical Study of the Effects of a Corotating Interaction Region on Cosmic-Ray Transport: Some features of different Cosmic-Ray Composition and Rigidity

Xi Luo,[a,*] **Marius Potgieter,**[a,b] **Ming Zhang,**[c] **Fang Shen,**[d] **Mikhail Krainev,**[e] **Galina Bazilevskaya**[f] **and Vladimir Mikhailov**[g]

[a] *Shandong Institute of Advanced Technology (SDIAT), 250100 Jinan, Shandong, PR China*
[b] *Institute for Experimental and Applied Physics (IEAP), Christian-Albrechts University in Kiel, 24118 Kiel, Germany*
[c] *Department of Physics and Space Sciences, Florida Institute of Technology, Melbourne, FL 32901, USA*
[d] *SIGMA Weather Group, State Key Laboratory of Space Weather, National Space Science Center, Chinese Academy of Sciences, Beijing 100190, PR China*
[e] *Lebedev Physical Institute of Russian Academy of Sciences, Russia*
[f] *Lebedev Physical Institute of Russian Academy of Sciences, Russia*
[g] *National Research Nuclear University MEPhI (Moscow Engineering Physics Institute), Russia*

E-mail: xi.luo@iat.cn, marius.s.potgieter@gmail.com

Recently, with Galactic Cosmic Ray (GCR) observations available from the state-of-the-art space experiments (AMS-02, PAMELA, et.al.), the solar modulation of these particles has been studied on different time scales over a wide rigidity range. A clear 27-day-periodicity is confirmed in the fluxes of protons and revealed for GCR helium. It is well known that Corotating Interaction Regions (CIRs) are the main driver for this periodicity. In this study, using a hybrid MHD-GCR transport numerical model, we investigate CIR effects on helium and proton fluxes close to the Earth. It was found that: Protons and the two helium isotopes are modulated differently by a CIR; as expected the magnitude of this decrease varies with GCR rigidity.

38th International Cosmic Ray Conference (ICRC2023)
26 July - 3 August, 2023
Nagoya, Japan

*Speaker

PoS(ICRC2023)1241

1. Introduction

Based on various observation [1, 7, 8], i.e. ground neutron monitors (NMs), Spacecrafts, it is known that GCR intensity measured near the Earth displays 27 days periodic variations. The GCR 27 days periodic variations usually occur at the times of solar mimima. The 27 day variations of GCRs are observed near Earth by many space missions (e.g., IMP8, Richardson et al. [11]; ACE, Leske et al. [4]; and others[1, 9]), in the inner heliosphere. As recently reported by [5, 9, 12], the CIR, caused by the interaction between fast solar wind and slow solar wind, is the main driver for the 27 days intensity variation of GCRs.

CIR also serves as a significant source of energetic particles in the interplanetary medium. While shock acceleration has historically been viewed as a main acceleration mechanism at CIRs, some studies have indicated the importance of particle acceleration mechanisms within 1 au such as stochastic processes [2] or processes in the unshocked compression region due to the velocity gradient across the CIR [3].

In this study, we contine our previous study of the CIR effects on GCR transport [5]. And the focus here is on the characteristcs related to the GCR composition and rigidty . In the following, we will disucss our numerical model brefly and then present some of the simulation results with a short disucssion.

2. Numerical Model

The numerical model used in current study is essentially the same as our investigation before [5]. The Magnetohydrodynamic (MHD) model is adapted to resolve the plasma background in the inner heliosphere. We still utilize the MHD simulated plasma profile for Carrington Rotation 2066 (Jan. 2008), which corresponds to a solar mimimum phase of solar cycle 23. The details of the MHD model and the plasma profile have already been reported previous [5, 6].

It should be mentioned that the MHD simulation is carried out in the solar co-rotating frame, and it only resolve the plasma profile up to about 27 au. As for the outter heliosphere with radial distance larger than 27 au, the Parker Interplanetary Magnetic Field (IMF) model is utilized. Additionally, with the following setup for plasma speed and interplanetary magnetic field, a simplified termination shock model is included in our numerical model.

$$\begin{aligned} \mathbf{V}_{sw} &= V_{r0}(1/C_r)(\frac{r_{ts}}{r})^2\hat{e_r}, \\ b_r &= b_{r0}(\frac{r_{\rm in}}{r})^2 C_r, \\ b_\theta &= b_{\theta 0}(\frac{r_{\rm in}}{r_{\rm ts}})C_r(\frac{r}{r_{\rm ts}}), \\ b_\phi &= b_{\phi 0}(\frac{r_{\rm in}}{r_{\rm ts}})C_r(\frac{r}{r_{\rm ts}}) \end{aligned} \tag{1}$$

Here, $\mathbf{V}_{r0}, b_{r0}, b_{\theta 0}, b_{\phi 0}$ are the solar wind radial component, IMF radial, polar and azimuthal components at the upstream of the TS. C_r is the TS shock compression ratio, which is set as 3.3 and $r_{\rm ts}$ = 92 au, the radial distance location of the TS, with $r_{\rm in}$ = 130 au, the location of the our GCR

transport simulation outer boundary. Note the plasma background outer boundary is set at 145 au, which is roughly beyond the GCR transport region.

The solar wind plasma flow is treated as an incompressible plasma fluid, thus $\nabla \cdot \mathbf{V}_{sw} = 0$. Due to the shock compression, the magnetic field increases beyond the TS.

It is known that the very Local Interstellar Spectra (LIS), which is set as the outter boundary condition for GCR transport simulation, and the mass-charge-ratios are different for He-3 and He-4. To correctly model the GCR Helium tranport inside the heliosphere, the very LIS's for He-3 and He-4 need to be separated [10].

As for the GCR transport model, it is based on the Parker Transport Equation (PTE). Following our previous work [5], its Stochastic Differential Equation (SDE) form is utilized to.

$$d\vec{X} = (\nabla \cdot \mathbf{K}_s - \mathbf{V}_{sw} - \mathbf{V}_d)ds + \sum_{\sigma} \vec{\alpha_\sigma} dW_\sigma(s) \quad , \tag{2}$$

$$dp = \frac{1}{3} p (\nabla \cdot \mathbf{V}_{sw}) ds \quad . \tag{3}$$

In the following, the diffusion coefficient and drift velocity form, which is used in our numerial model, will be brifely described. $K_\parallel, K_\perp$ in $\mathbf{K}_s$ are given by the following equations:

$$K_\parallel = K_0 \beta \left(\frac{B_{eq}}{B}\right) \left(\frac{R}{R_0}\right)^a \left(\frac{\left(\frac{R}{R_0}\right)^c + \left(\frac{R_k}{R_0}\right)^c}{1 + \left(\frac{R_k}{R_0}\right)^c} \right)^{\frac{b-a}{c}} \quad , \tag{4}$$

and

$$K_\perp = 0.02 K_\parallel . \tag{5}$$

The drift velocity is given by :

$$\langle \vec{v_D} \rangle = (K_d)_0 \frac{pv}{3q} \nabla \times (\frac{\vec{B}}{B^2}) = (K_d)_0 \frac{\beta R}{3} \nabla \times (\frac{\vec{B}}{B^2}), \tag{6}$$

with q the charge of particles, p particle momentum, R particle rigidity. $(K_d)_0$ is a dimensionless parameter, which sets how the drift velocity is reduced.

3. Simulation Results

Figure 1 illustrates the flux variations of proton, He-3 and He-4 at 3 au with longitude inside a typical CIR event. The plasma background characteristics, such as the solar wind speed (V_{sw}), magnetic field magnitude (B) and plasma density (N) are plotted as a function of longitude in the upper panels (A, B, C). The longitudinal variation of the respective fluxes are demonstrated in the lower three panels (D, E, F). The solid line denotes the 0.3GV case, while the dotted line denotes the 1.7GV case.

Since the CIR is almost steady state during several solar rotational period, in the solar co-rotating frame, the GCR intensity variation in longitude reflects how the GCR intensity observed near Earth vary with time during the Carrington Rotation period. According to the simulated plasma characteristics, at around 180° heliolongitude, the magnetic field magnitude and plasma density

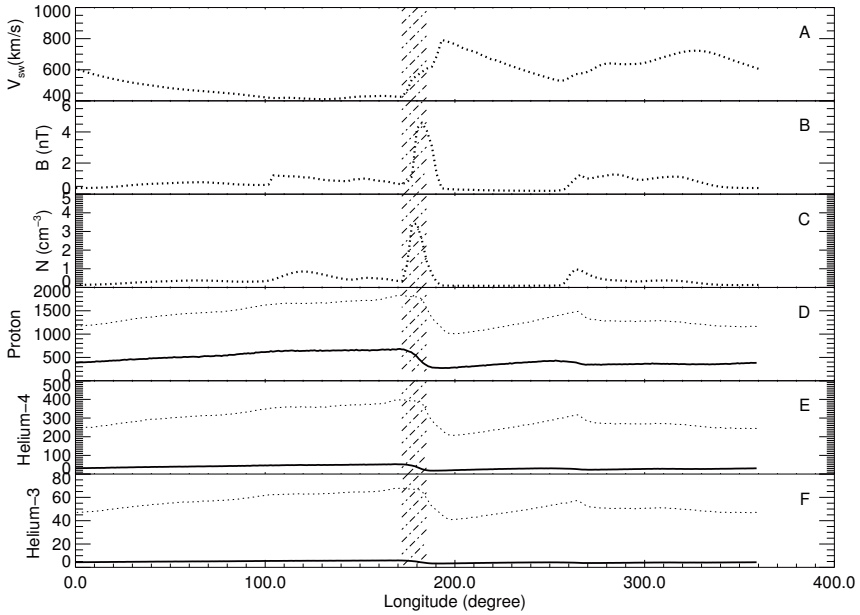

Figure 1: The plasma background characteristics, solar wind speed (Vsw), magnetic field magnitude (B) and plasma density (N), are plotted as a function of heliolongitude in the upper panels (A,B,C) together with the simulated 0.3 GV (solid line), 1.7 GV (dotted line) flux for protons, Helium-3 and Helium-4 at 3.01 au in the lower panels (D,E,F). The units for the GCR flux is 1/(m2/sr/s/(GeV/n)). Shaded range indicates where the solar wind plasma is compressed between fast and slow streams.

reach a peak value, indicating that the solar wind plasma is compressed between fast and slow solar wind streams. This is highlighted with a shaded range, which indicates the simulated CIR as it follows from the MHD model. It is illustrated by panels D, E, F that inside the CIR the three GCR fluxes, for protons, He-3 and He-4, experience a significant depression. This scenario is consistent with the current understanding of how the CIR affects GCR transport [13]. Illustrated by Figure 1, the magnitude of the flux depression level is much less for 1.7 GV case.

Additionally, as demonstrated by figure 2 and figure 3, the proton and helium-4 flux longitude variation depends on rigidity as well. Obviously, GCR rigidity is an important characteristic for its transport inside the CIR, and the CIR effects for proton tranport closely relate to proton rigidity. It is well known that there are four major machansim for GCR transport, e.g. diffusion, drift, convection and adiabatic cooling. In the numerical model we used, only diffusion and drift processes relates to the rigidity, if we can disentangle the two processes and reveal its relationship with rigidity, some knowledege about the diffusion and drift processes can also be gained.

4. Summary

As recent GCR observation for its short term variation, e.g, solar rotational period, become avaiable [1, 9]. Some new features of its 27 day variation has been revealed, such as its relationship with GCR composition, rigidity, charge etc. In this circumstance, corresponding numerical model has also been developped. The hybrid model that we developped contains a MHD model for the inner heliosphere, and the Parker transport equation is utilized to simulate the GCR transport

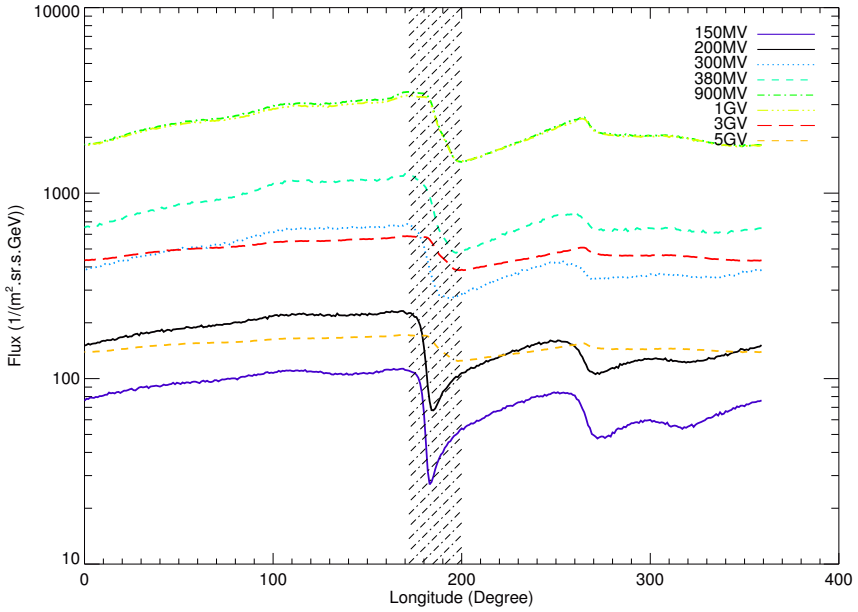

Figure 2: Simulated proton flux variation with longitude for eight different rigidity levels at 3 au. The X-axis is longitude, which represents the flux variation with time in one Carrington Ration period.

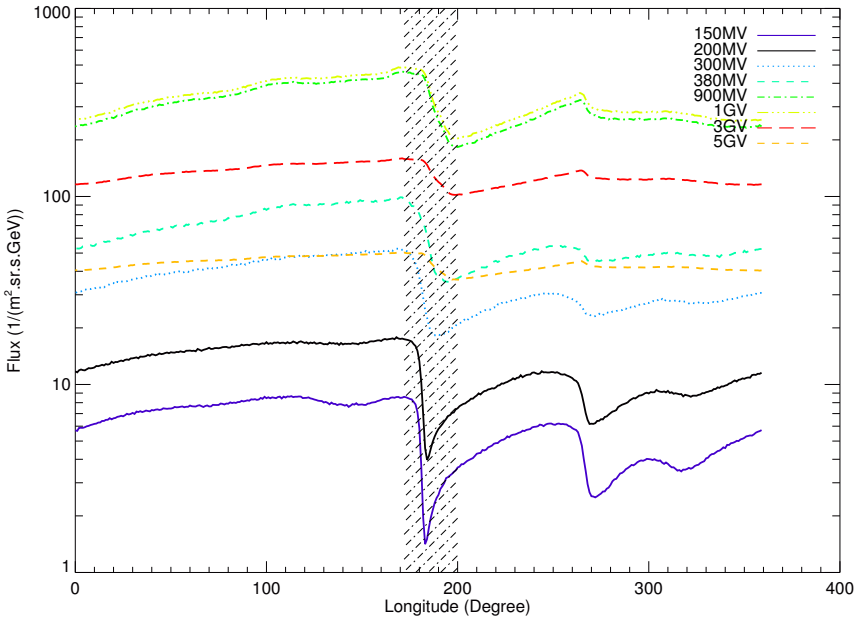

Figure 3: Simulated helium-4 flux variation with longitude for eight different rigidity levels at 3 au. The X-axis is longitude, which has the similar layout with figure 2.

processes in the interplanetary space. Additionally, the helium-4 and helium-3 local interstellar spectrum have been seperated to simulate the helium isotopes transport processes.

Our numerical model simulation results have revealed that both protons and helium isotopes are modulated by the CIR, their intensity depresses inside the CIR. Additionally, as our simulation revealed, the CIR effect relates to GCR rigidity. Either proton or helium, the depression magnitude is larger for lower rigidity GCR. It implies that the GCR transport physical processes inside the CIR should relate to GCR rigidity. By exploring this feature further, some insights for the transport processes can be gained.

References

[1] Aguilar, M., Cavasonza, L., Ambrosi, G., Arruda, L., Attig, N., et al. 2021, Physical Review Letters, 127, 271002

[2] Chotoo, K., Schwadron, N. A., Mason, G. M., Zurbuchen, T. H., et al., 2000, J. Geophys. Res., 105, A10

[3] Chen, B., Bastian, T. S., Shen, C., et al., 2015, Science, 350, 1238.

[4] Leske, R., Cummings, A. C., Mewaldt, R. A., et al. 2011, 32nd International Cosmic Ray Conference, 11, 194

[5] Luo, X., Zhang, M., Feng, X., et al. 2020, The Astrophysical Journal, 899, 90

[6] Luo, X., Feng, X., Shen, F., et al. 2022, 37th International Cosmic Ray Conference, 1353.

[7] Kunow, H., Dröge, W., Heber, B., et al. 1995, Space Science Reviews, 72, 397

[8] Gil, A., & Alania, M. V. 2016, solar physics , 291, 1877

[9] Modzelewska, R., Bazilevskaya, G.A., Boezio, M. et al. 2020, The Astrophysical Journal, 904, 3

[10] Ngobeni, M.D., Aslam, O.P.M., Bisschoff, D. et al. 2020, Astrophys Space Sci, 365, 182

[11] Richardson, I. G., Wibberenz, G., & Cane, H. V. 1996, JOURNAL OF GEOPHYSICAL RESEARCH, 101, A6, 13483

[12] Richardson, I. G. 2004, Space Science Reviews, 111, 267

[13] Richardson, I. G. 2018, Living Rev Sol Phys, 15, 1